Homeostatic control of Argonaute stability by microRNA availability

Peter Smibert, Jr-Shiuan Yang, Ghows Azzam, Ji-Long Liu and Eric C. Lai

Supplementary Figures 1-6

Supplementary Figure 1. Accumulation of AGO1 protein depends on the core miRNA biogenesis factor Dicer-1 in ovarian germline cells.

- Relevant to Main Figure 1.

Supplementary Figure 2. Accumulation of AGO1 protein depends on the core miRNA biogenesis machinery in the larval brain.

- Relevant to Main Figure 1.

Supplementary Figure 3. The RING finger protein Mei-P26 is an endogenous miRNA target that is universally de-repressed in miRNA pathway mutant conditions, but does not influence AGO1 levels.

- Relevant to Main Figure 1.

Supplementary Figure 4. Examination of Ago1 stability in Dicer-KO MEFs.

- Relevant to Main Figure 4.

Supplementary Figure 5. Roles of autophagy and Hsp90 in Argonaute stability.

- Relevant to Main Figure 4.

Supplementary Figure 6. Uncropped Western and Northern blots for all data presented in the Main Figures.

- Relevant to Main Figures 2, 4 and 5.

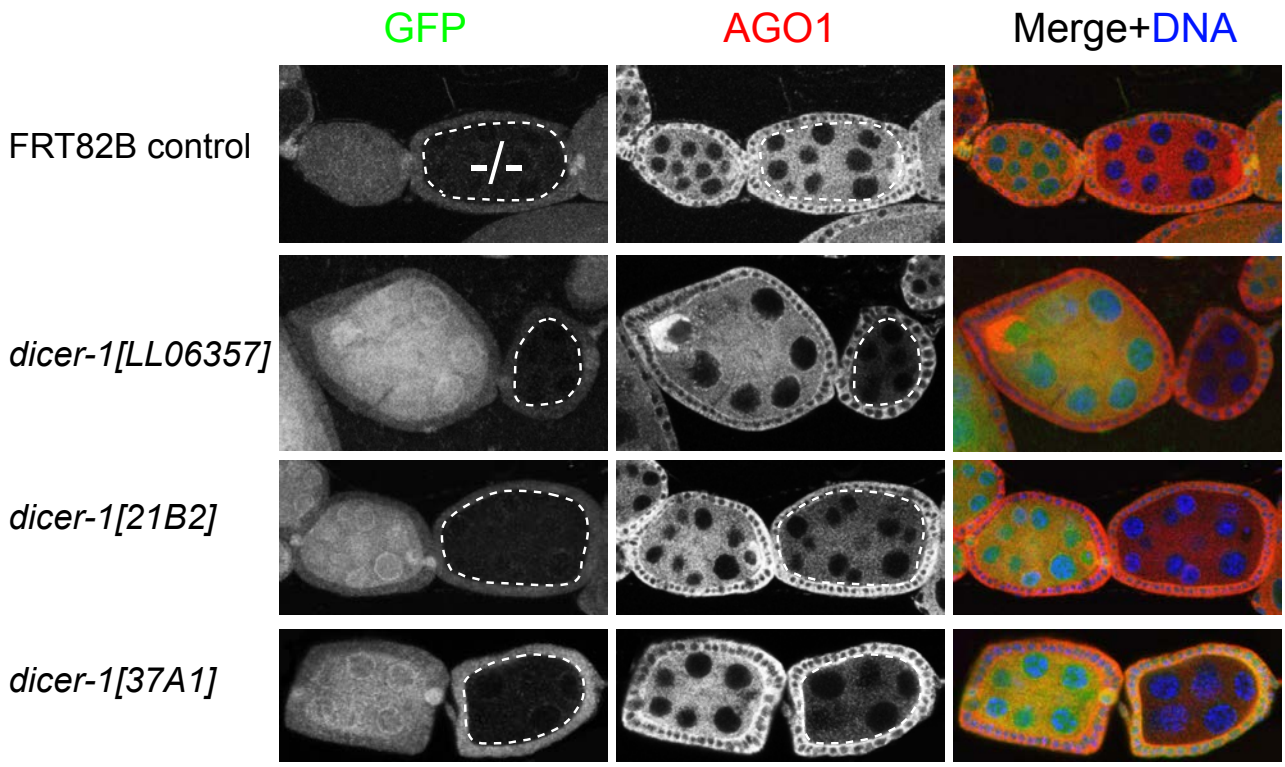

Supplementary Figure 1. Accumulation of AGO1 protein depends on the core miRNA biogenesis factor Dicer-1 in ovarian germline cells. Egg chambers bearing negatively marked germline mutant clones lacking GFP expression (dotted lines, "-/-") were stained for AGO1 protein. The levels of AGO1 in mutant egg chambers (oriented to the right of each pair) can be directly compared with neighboring GFP+ egg chambers. FRT82B control clone shows no change in AGO1, whereas AGO1 is depleted in three different *dicer-1* mutant germlines.

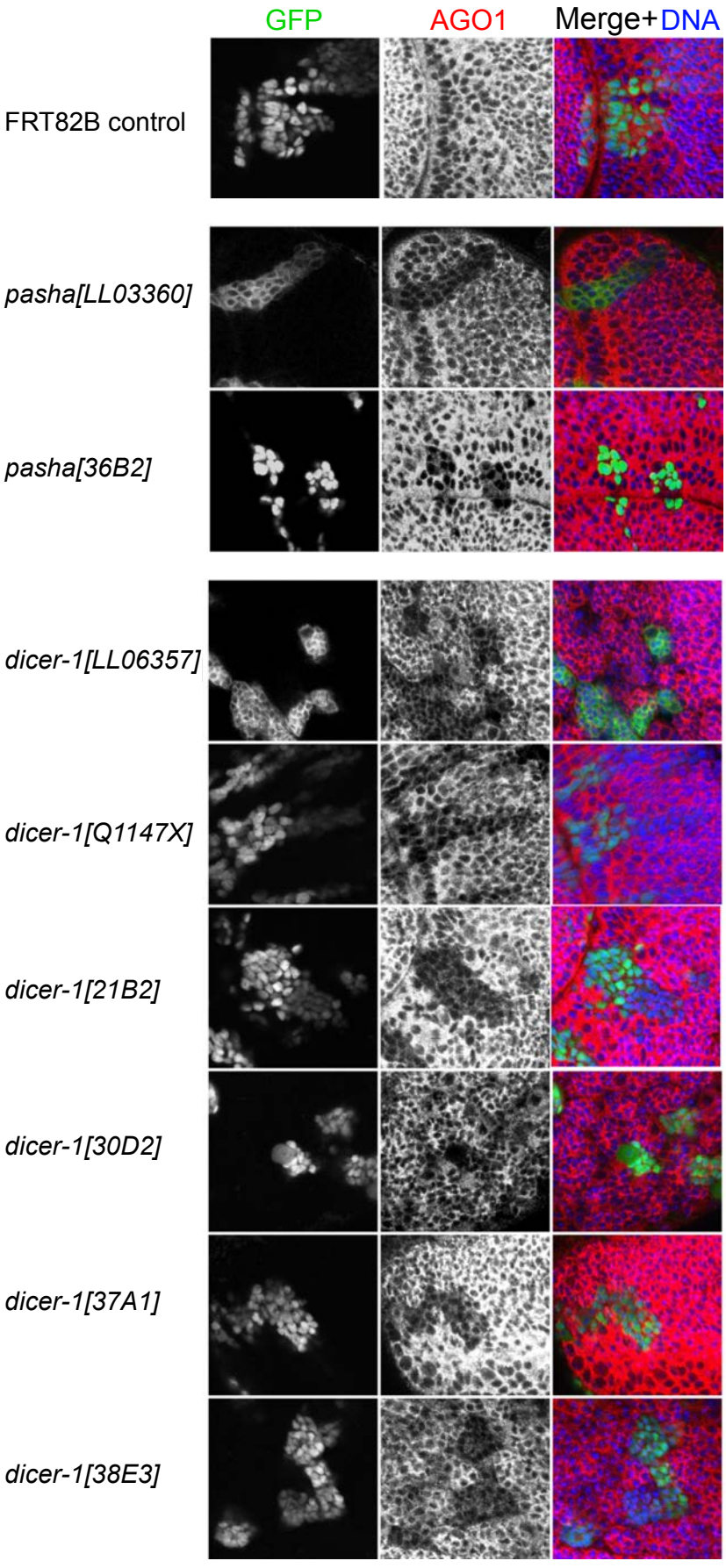

Supplementary Figure 2. Accumulation of AGO1 protein depends on the core miRNA biogenesis machinery in the larval brain. MARCM mutant clones positively labeled by GFP (green, left column of panels in grayscale) were stained for AGO1 protein (red, middle column of panels in grayscale); merged images are shown in the right column of panels (counterstained with DAPI in blue). No alteration of AGO1 protein is seen in control FRT82B MARCM clones, whereas AGO1 is depleted in two *pasha* alleles, or any of six different *dicer-1* alleles.

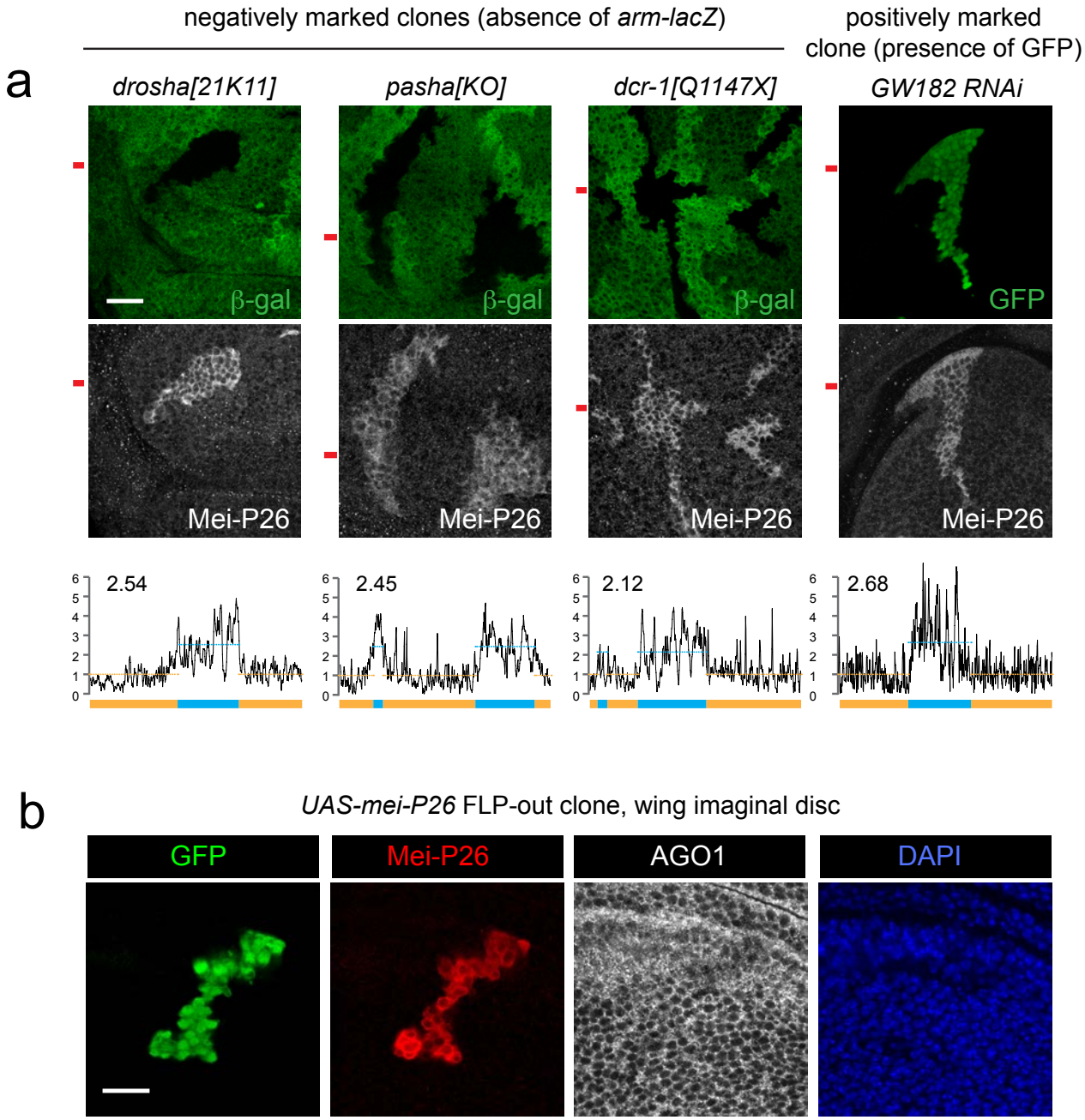

Supplementary Figure 3. The RING finger protein Mei-P26 is an endogenous miRNA target that is universally de-repressed in miRNA pathway mutant conditions, but does not influence AGO1 levels.

(a) Wing imaginal disc clones that are negatively marked by absence of ß-galactosidase, or positively marked by GFP; these were all co-stained for Mei-P26. Clones homozygous for null alleles of the core miRNA biogenesis factors *drosha*, *pasha*, *dcr-1*, or that express RNAi against GW182, all de-repress Mei-P26 to a similar extent. The graphs below depict confocal pixel intensities across the single slices marked by the red lines. The location of control and mutant sectors are marked by yellow and blue boxes, respectively. The level of Mei-P26 accumulation in all of these miRNA pathway mutant conditions is comparable. Note that the *GW182-RNAi* clone data in this figure are presented in modified form in main Figure 1c, and are shown here to facilitate direct comparison with the *drosha*, *pasha*, and *dcr-1* clone data. Scale bar = 20μm.

(b) Wing disc clone misexpressing Mei-P26 (marked by GFP, green) exhibits highly elevated Mei-P26 protein (red), but AGO1 protein is unaltered (gray). Nuclei are labeled by DAPI (blue). Scale bar = 20μm.

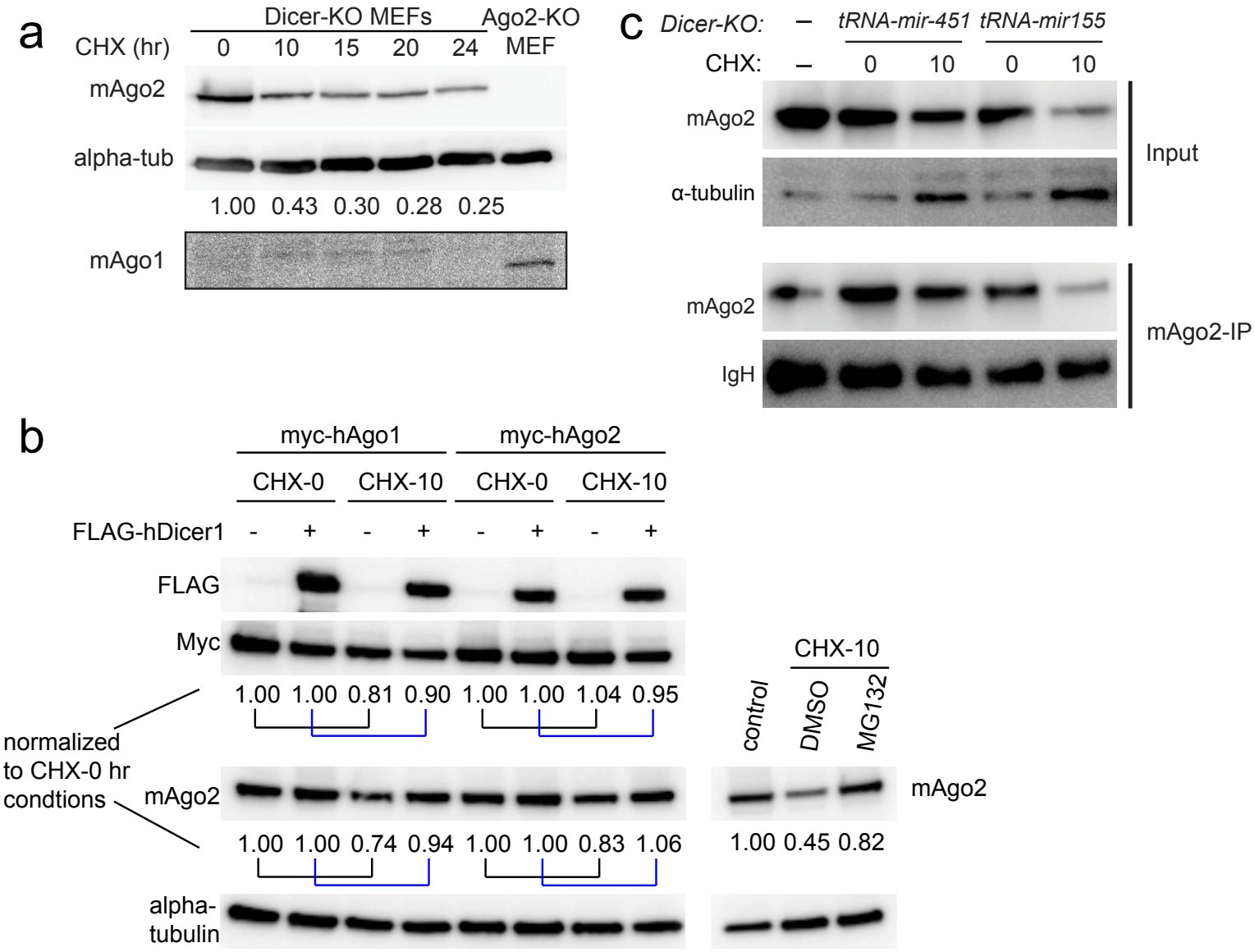

Supplementary Figure 4. Examination of Ago1 stability in Dicer-KO MEFs. (a) Dicer-KO MEFs were treated with cycloheximide and harvested at indicated times. Levels of mAgo2 were gradually decreased over the 24h-treatment. Specificity of the signal is shown by its absence from Ago2-KO MEFs. Note that no mAgo1 protein was detected in the Dicer-KO MEFs. The efficacy of the mAgo1 antibody was validated by the signal from the Ago2-KO MEFs. (b) Dicer-KO MEFs were cotransfected with myc-tagged hAgo1 or hAgo2 and FLAG-tagged hDicer1 for 24h and then treated with cycloheximide for 10h. No obvious difference in levels of myc-hAgo2 was detected in the presence of cycloheximide for 10h compared to 0h. Moreover, the decay of endogenous mAgo2 was slowed by the expression of both myc-hAgo1 and myc-hAgo2 proteins, suggesting that the presence of ectopic Ago proteins disrupted the turnover of endogenous Ago2 proteins. The efficacy of cycloheximide treatment was confirmed by the non-transfected Dicer-KO MEFs.
(c) Rescue of mAgo2 level in Dicer-KO MEFs by Dicer-independent miRNAs. Transfection of tRNA-mir-451, but not by tRNA-mir-155, increased the stability of mAgo2 as assessed in total cell extracts and in mAgo2-IPs.

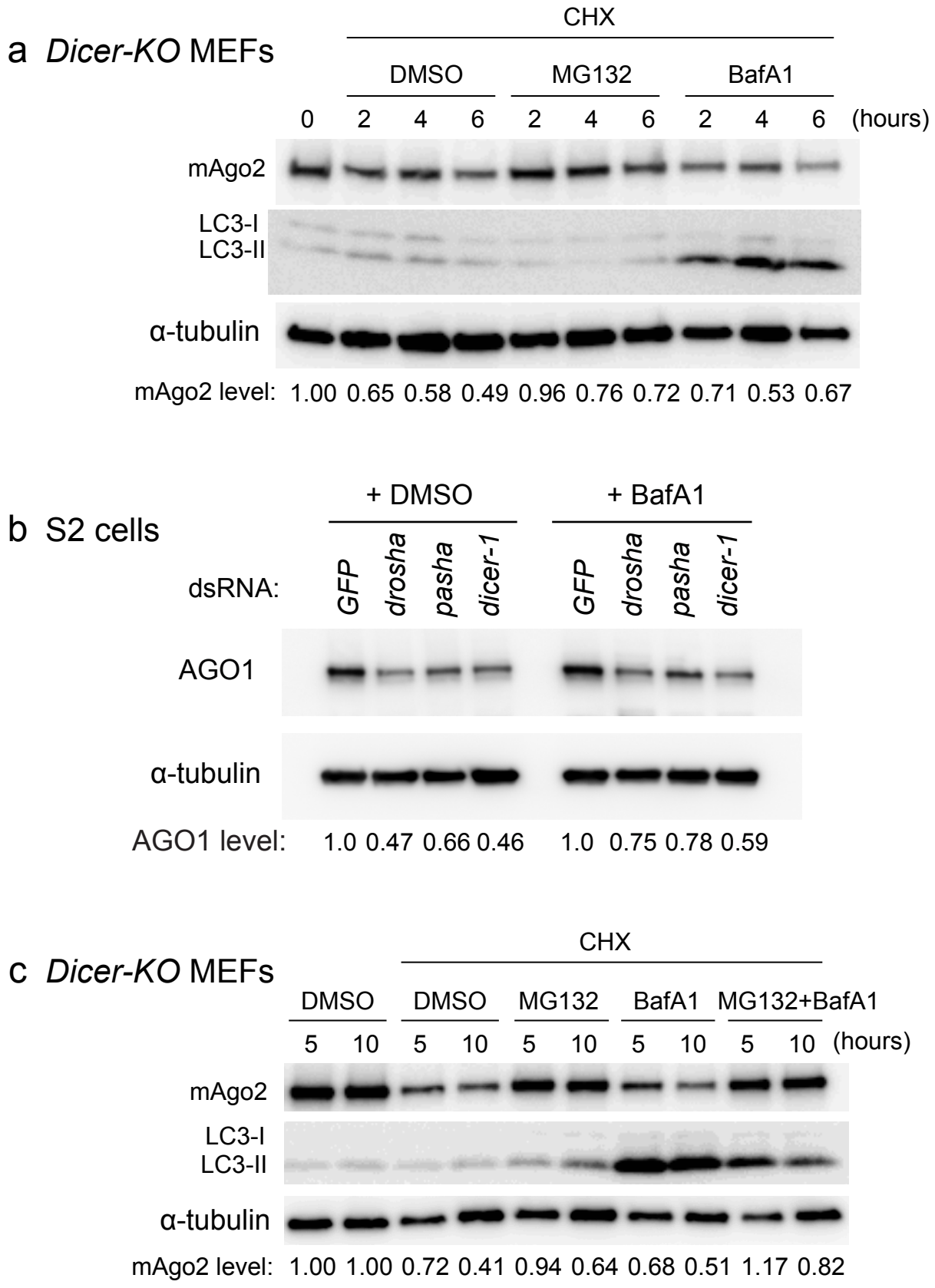

Supplementary Figure 5. Roles of autophagy and Hsp90 in Argonaute stability. (a) Dicer-KO MEFs were treated with Cycloheximide and either DMSO, MG132 or Bafilomycin A1 for the indicated times. A mild stabilizing effect on mAgo2 was observed for MG132 but no obvious difference in mAgo2 stability was observed following BafA1 treatment. The accumulation of LC3-II demonstrates the effectiveness of the BafA1 treatment. (b) S2 cells previously subjected to 2x4 days of soaking with the indicated dsRNAs were treated with either DMSO or Bafilomycin A1 for 4 hours. No clear rescue of AGO1 stability was observed.
(c) Cotreatment of MG132 and BafA1 led to a slight increase in mAgo2 levels compared to MG132 alone.

Figure 2a

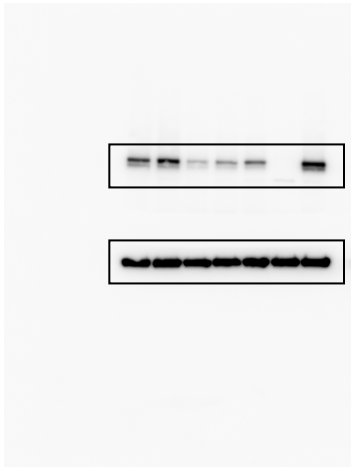

Figure 2b

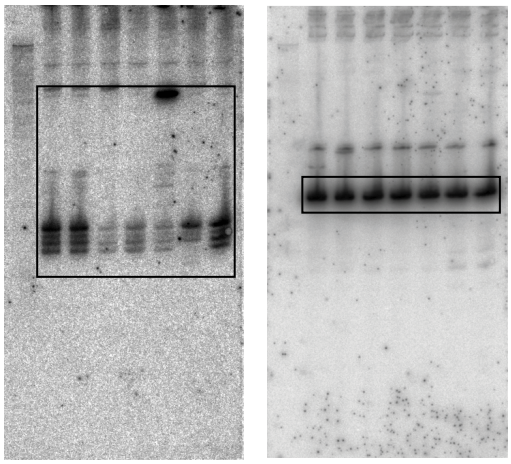

Figure 2e

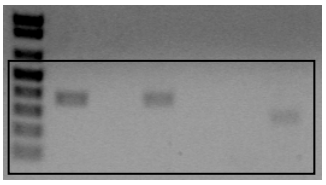

Figure 2f

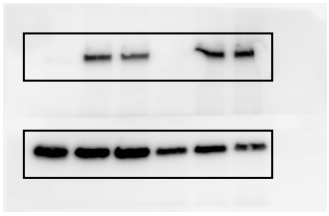

Figure 4b

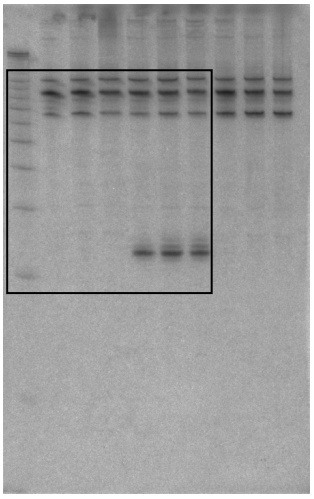

Figure 4c

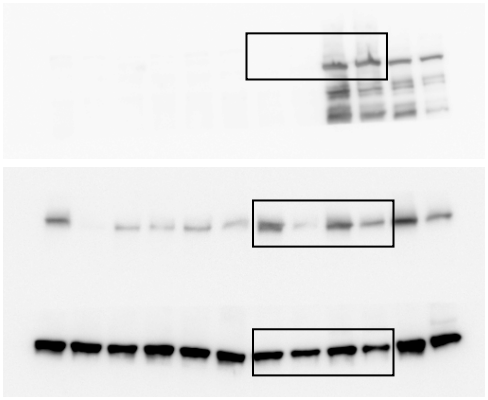

Figure 4e

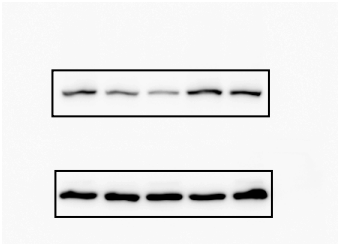

Figure 4f

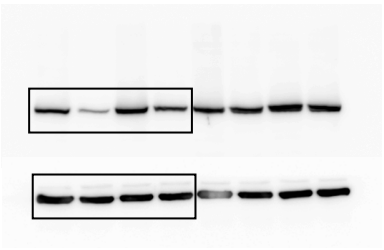

Figure 5a

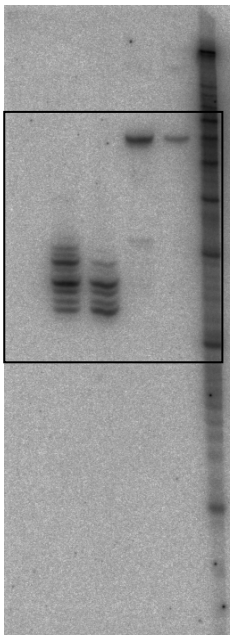

Figure 5b

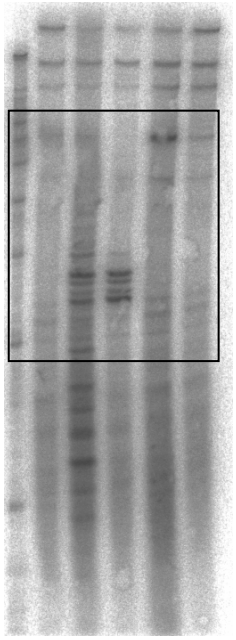

Figure 5c

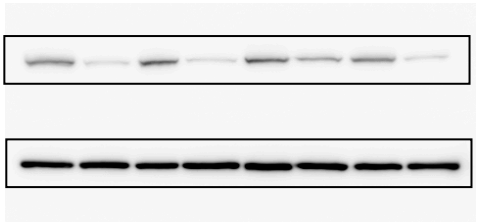

Figure 5e

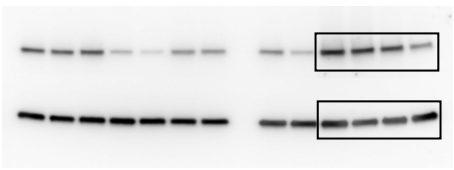

Figure 5d

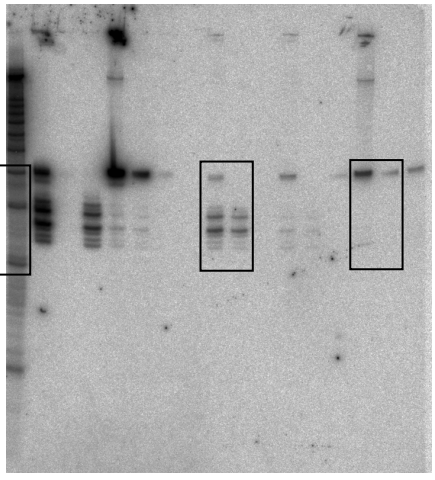

Figure 5g

Supplementary Figure 6. Uncropped Western and Northern blots for all data presented in the Main Figures.